

Article

Fabrication of Superhydrophobic Metallic Surface by Wire Electrical Discharge Machining for Seamless Roll-to-Roll Printing

Jin-Young So and Won-Gyu Bae *

Department of Electrical Engineering, Soongsil University, Seoul 156-743, Korea; igiyou@ssu.ac.kr

* Correspondence: wgbae@ssu.ac.kr; Tel.: +82-2-820-0655

Received: 25 February 2018; Accepted: 30 March 2018; Published: 2 April 2018



Abstract: This paper presents a proposal of a direct one-step method to fabricate a multi-scale superhydrophobic metallic seamless roll mold. The mold was fabricated using the wire electrical discharge machining (WEDM) technique for a roll-to-roll imprinting application to produce a large superhydrophobic surface. Taking advantage of the exfoliating characteristic of the metallic surface, nano-sized surface roughness was spontaneously formed while manufacturing the micro-sized structure: that is, a dual-scale hierarchical structure was easily produced in a simple one-step fabrication with a large area on the aluminum metal surface. This hierarchical structure showed superhydrophobicity without chemical coating. A roll-type seamless mold for the roll-to-roll process was fabricated through engraving the patterns on the cylindrical substrate, thereby enabling to make a continuous film with superhydrophobicity.

Keywords: superhydrophobicity; dual-scale roughness; wire electrical discharge machining

1. Introduction

Recently, microelectromechanical systems (MEMS) and nanoelectromechanical systems (NEMS) technology has been rapidly developing due to recently introduced semiconductor techniques. Consequently, biomimetics, which imitates the systems of nature, is also developing rapidly using these semiconductor techniques [1–4]. The biomimetic technique is currently attracting considerable attention, probably for its use in lotus leaf surface imitation. The micro-sized structure of the lotus leaf has a surface with nano-sized bumps, which is called a dual-scale roughness patterned surface [5,6]. The lotus leaf has many advantages due to these morphological features, the most renowned feature being its superhydrophobic properties. This means the surface is not made wet by water; thus, if it rains, water easily falls off the surface, providing a self-cleaning effect. This unique feature has value not only for academic study but also for use in various industrial fields through commercialization. Several attempts to imitate the multi-scale structure of this surface are therefore being carried out.

Until now, superhydrophobic methods have largely been divided into two types: the bottom-up method and the top-down method. These two major methods are used to create nanoscale structures. The bottom-up method seeks to molecularly build up into more complex nanoscale assemblies based on complex technologies. In some studies, hydrophobic surfaces have been fabricated with nano-sized silica particles using the sol-gel method and with carbon nanotubes (CNTs) through the bottom-up method. Alternatively, the top-down method corresponds to using nanofabrication tools to produce nanoscale structure devices with the desired shapes starting from larger dimensions. For the top-down method, rough irregular surfaces have been made using the argon ion collision and oxygen plasma etching methods with materials such as polytetrafluoroethylene (PTFE) with hydrophobic features [7,8]. However, the disadvantage of these methods is their low reproducibility, and it is difficult to control

the hydrophobic degree precisely. Other studies have realized and controlled the hydrophobicity of surfaces by using the top-down method and photolithography used to produce micro/nanofabrication mostly for MEMS processing. A microstructure of the desired size is made first using the traditional lithography process, and the nano pattern of the desired size is then made using various non-traditional nano-patterning techniques on the surface to obtain the hydrophobic surface. Since these methods are based on the traditional lithography method, they have good reproducibility, and the surface shape can be controlled as desired. However, as the surfaces are based on solid wafers, it is difficult to realize surfaces beyond the wafer size, the processing time and cost are high, and they do not bend. In addition, the structures of surfaces made in this way are easily broken, so the functionality of the surfaces cannot be guaranteed for a long period of time. These surfaces are also difficult to apply in real industries.

Apart from these two methods, another manner of fabricating the hydrophobic surface via laser ablation is also employed. Using a laser, the surface can be made with the hydrophobic properties by generating the precise pattern on the surface. However, it is economically inefficient to fabricate the surface with these hydrophobic properties by simply making a random microstructure or surface, due to the expensive laser device.

In this study, a simple and large-scale patterning method was realized by direct patterning on the metal surface using wire electrical discharge machining (WEDM), a metal processing method, in order to produce the micro/nanostructure in one-step fabrication. WEDM is widely used in the metal processing field and is a precise processing technique that can create shapes on surfaces in numerous micro-units [9–14]. Moreover, since the WEDM process induces discharge on the metal surface during processing, the nano-sized roughness is automatically created, and the multi-scale shape can be obtained in one step. If the surface has this multi-scale structure, superhydrophobic surfaces could be obtained comparatively easily due to the lotus effect, where the leaves of the lotus flower exhibit hydrophobicity [15–17].

Functional films can be made by reproducing this multi-scale structure on the film; the roll-to-roll process is essentially used for mass production. However, in the past, the film on which the pattern was carved was rolled and attached to the roll to proceed with the roll-to-roll process. However, the disadvantage of this method is that the roll and attached film are reproduced together. EDM can process the cylindrical shape without seams, making it possible to process a seamless multi-scale patterned roll by processing a cylindrical roll of 45 mm in diameter while simultaneously conducting multi-scale patterning on the surface. The purpose of the current research was to contribute to describing the application of the wire electrical discharge machining (WEDM) and to make the multi-scale structure patterned polymer film in relation to the processes that have advantages of producing the large-scale and the seamless superhydrophobic polymer film through this metallic roll. This production method that allows superhydrophobicity to take place conveniently on the surface will lead to an increased WEDM application to transform the surface properties.

2. Materials and Methods

This research used a commercially available aluminum (Al) 7075 alloy (duralumin). The Al 7075 alloy comprises Al (87.1–91.4%), Mg (2.10–2.90%), Cu (1.20–2.0%), Fe (<0.50%), Si (<0.40%), Mn (<0.30%), Ti (<0.20%), Cr (0.18–0.280%), and Zn (5.10–6.10%). Table 1 shows chemical composition of the Al 7075 alloy. This Al alloy is widely used in the structural components of automotive vehicles and aircraft owing to its high strength to weight ratio [18,19].

Table 1. Chemical composition of the Al 7075 alloy.

Al	Cr	Cu	Fe	Mg	Mn	Si	Ti	Zn
87.1–91.4%	0.18–0.280%	1.20–2.0%	<0.50%	2.10–2.90%	<0.30%	<0.40%	<0.20%	5.10–6.10%

A commercial WEDM system (EZ20S, Seoul Precision Machine Co., Ltd., Seoul, Korea) was used to fabricate nano-sized surface roughness with microgrooves. Table 2 presents technical parameters of the commercial WEDM system.

Table 2. Parameters of the commercial wire electrical discharge machining (WEDM) system.

Electrode	Brass Strip Thickness: 0.1 mm Width: 10 mm Feed Speed: 2 mm/s
Workpiece	Al 7075 alloy
Working fluid	Deionized water
Open gap voltage	+126 V / −80 V (Bipolar)
Frequency	12.8 kHz
Positive/Negative duration	28 us/50 us
Peak current	150 A

In the case of plate type Al, the 7075 alloy was cut to the size of 30 mm × 30 mm × 2 mm (length × width × thickness). In the case of the cylinder type Al, the 7075 alloy was cut to the size of 45 mm in diameter and 150 mm in length. A brass strip of 250 μm in diameter was loaded as an electrode and the wire-electrode-feeding system that was at a minimum speed of 2 mm/s constantly supplied an intact wire to minimize the shape errors caused by the electrode wear. During the machining process, deionized (DI) water as a dielectric fluid was used to the WEDM machine and the Al alloy was submerged in the dielectric fluid, where deionized water was injected between electrode and workpiece. For its process, a pulsed-type voltage was supplied to the machining gap (positive voltage: +126 V, negative voltage: −80 V, current: 150 A, positive duration: 28 μs, negative duration: 50 μs) to obtain a rough surface on the workpiece. The fabricating process started with skim cuts and a high potential difference were made with gradually reduced potential differences for a fine finish. Here, the micro-sized primary structure is created in the shape of a sinusoidal profile at a wavelength of 500 μm. Additional roughness is simultaneously naturally fabricated with crater-like patterns of a few micrometers, covering the entire Al alloy surface. Details of our process can be found in our previous result [20].

Figure 1 shows a PFPE (perfluoropolyether) replica produced through micro molding. The drops of UV-curable PFPE precursor (0.1–0.5 mL), purchased from Minuta Tech, Seoul, Korea, were distributed on the metal mold, and a polyethylene terephthalate (PET) film (50 μm) was brought into contact with PFPE precursor in order to use it as a supporting backplane. Subsequently, the assembly was exposed to UV light (350 nm) for 5 mins. After UV curing, the PFPE mold was removed from the metal mold and cured for 10 h at room temperature for complete curing.

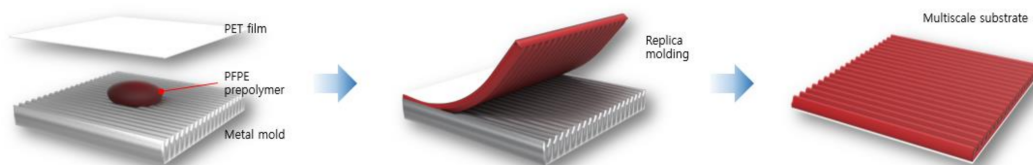


Figure 1. Fabrication scheme of perfluoropolyether (PFPE) replica replicated from the metal mold.

The static contact angles (CAs) and CA hysteresis of the liquids were measured using a DSA100 goniometer (Kruss, Hamburg, Germany). In each measurement, 5 μL of liquid was distributed on the surface over a time span of 1.5 min. The measurement was averaged over at least fifteen different locations for each sample condition.

Scanning electron microscopy (SEM) images were obtained using SEM (S-4800, Hitachi, Tokyo, Japan) at 15.0 kV and the working distance of 11.4 mm.

The multiscale rough metallic surfaces were directly mounted on a stage of non-contact three-dimensional (3D) surface profiler (NanoView-E1000; NanoSystem, Daejeon, Korea) shown in Figure 2 to acquire the average roughness and morphologic images. Images of $600\ \mu\text{m} \times 500\ \mu\text{m}$ area were acquired accordingly.

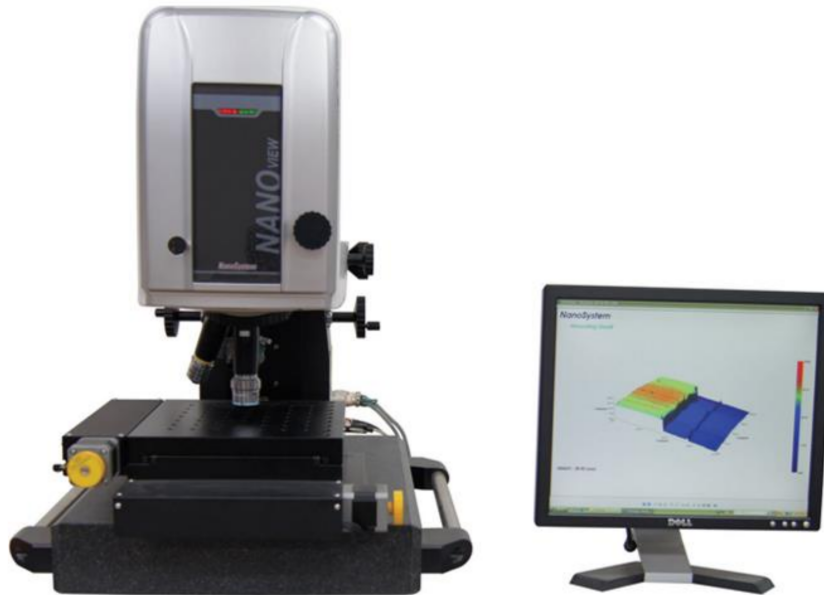


Figure 2. Non-contact three-dimensional surface profiler, NanoView-E1000.

3. Results and Discussion

3.1. Fabrication of Superhydrophobic Multi-Scale Roughness

It is well known that superhydrophobicity can be achieved by creating a hierarchical roughness on low surface energy-coated materials. Extensive studies have been conducted to mimic the lotus leaf using various smart methods, typically on polymeric materials [21–23]. Our understanding of the interplay between geometrical structures and surface chemistry has enabled the creation of superhydrophobicity on metallic surfaces. Metallic surfaces offer greater durability and robustness for harsh applications, including ships, automobiles, and aerospace engines [24,25]. Al alloys are used in many industrial applications due to their distinct properties, such as good mechanical properties, low corrosion resistance, and wide availability. Among these properties, it was found that Al alloys also have low surface energy ($\gamma = 30.65\ \text{mJ}/\text{m}^2$), which suggests even more applications. Also, it was observed that, because of the low surface energy of Al 7075 alloys, the creation of a microscale structure using WEDM can spontaneously induce a secondary roughness on the surface. The combination of low surface energy and hierarchical structures with single-step WEDM can be used to design metallic superhydrophobic surfaces [20]. WEDM is a non-traditional machining method for cutting metals. In the EDM process, applying a voltage to a wire electrode and a workpiece generates discharge sparks in the machining gap. Since the gap is very narrow, electrons can pass through the working fluid, causing sparks. Then, the high temperature and pressure produced by the sparks continuously melt and remove small portions of the surfaces of the wire electrode and the workpiece. Therefore, the machined surface of the workpiece consists of numerous craters that create the surface roughness.

Figure 3a illustrates a schematic simple wire electrical discharge machining (WEDM) process for fabricating dual-scale roughness (primary roughness: micro sinusoidal wavelength

pattern, secondary roughness: naturally generated craters on metal surface) on metallic surfaces with superhydrophobicity.

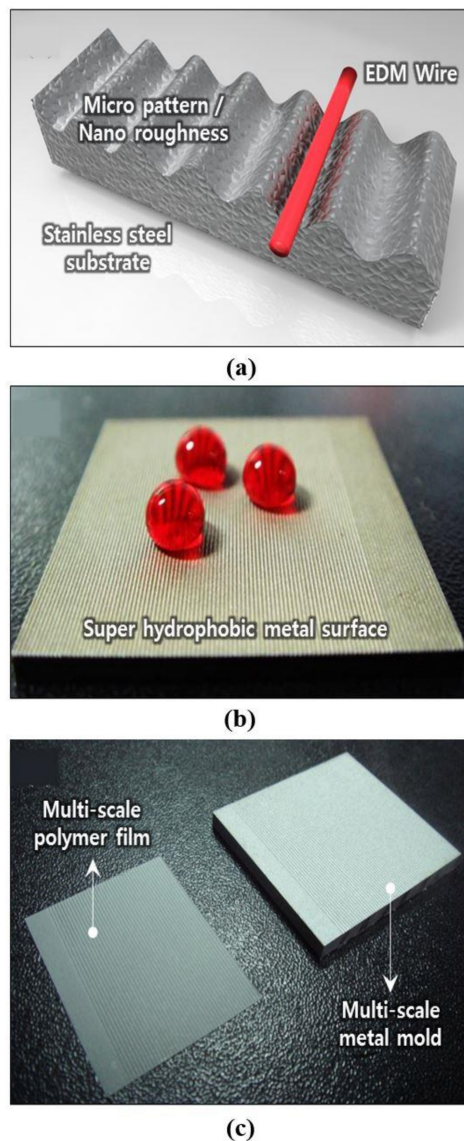


Figure 3. (a) Schematic diagram of fabrication of dual-scale structures on metallic surfaces by WEDM. Through single-step machining of sinusoidal patterns, an additional roughness is spontaneously generated owing to its surface exfoliation process; (b) Photograph of the multi-scale patterned aluminum surface demonstrating superhydrophobic properties ($\lambda = 500 \mu\text{m}$, Amplitude: $74 \mu\text{m}$, Roughness (R_a): $4.16 \mu\text{m}$); (c) To explain the concept, photograph of a replicated polymer film with multi-scale pattern.

The surface of Al with such roughness has hydrophobicity or water repellence, due to a combination of low surface energy (a unique characteristic of the material) and a structural characteristic of roughness. This is the same as the lotus effect, where the leaves of the lotus flower exhibit hydrophobicity.

When the surface of Al is cut once by WEDM, the highest average roughness (R_a : $4.16 \mu\text{m}$) is obtained. The recurrent machining of the surface thus cut produces an increasingly lower average roughness: $2.37 \mu\text{m}$ for the second time, $0.94 \mu\text{m}$ for the third time, and $0.41 \mu\text{m}$ for the fourth time.

In addition, as the roughness reduces, the contact angle also reduces; the contact angle was 156.5° at the first cutting, then 140.3° on the surface with the fourth cutting. This phenomenon can be explained by the renowned Cassie–Baxter models. In this model, if a sufficient number of voids are formed due to a rough surface when the water droplet contacts the rough surface of the solid, the contact area between the solid and the droplet is reduced. It can therefore be seen that the water contact angle is increased. That is, as the surface roughness increases, hydrophobicity appears on the surface.

$$\cos\theta_C^* = -1 + f(\cos\theta + 1) \quad (1)$$

where θ_C^* is the Cassie–Baxter CA with a rough surface, θ is a CA with a flat surface, and f is a roughness factor defined as the ratio between the actual droplet contact area and the total surface area.

In the metallic multi-scale structure made in this study, θ was 109° , and θ_C^* was 156.5° at the first cutting, so f can be calculated as 0.78. At the fourth cutting, θ_C^* was 140.3° , and accordingly the value of f is 0.83. That is, it can be confirmed that as the surface roughness increases, the value of f decreases, implying the reduction of the ratio of contact between the solid surface and the water. In other words, the water droplet is supported by the air in the space of the macro/nano structure. Therefore, it is demonstrated that the role of the micro/nano structure is important to obtain a hydrophobic surface with better properties.

Meanwhile, as shown in Figure 3b, a structure with a scale of hundreds of micrometers ($\lambda = 500 \mu\text{m}$) was fabricated on the surface of Al and a multi-scale structure with spontaneously generated several nanometer roughness was also made. The Al surface thus fabricated shows a superhydrophobic characteristic ($\text{CA} > 156 \pm 5^\circ$). As revealed in the conclusions of numerous preceding studies, the requirements of both structural and chemical features need to be met in order to obtain the superhydrophobic property. However, this study proposes an easy and simple method of producing a superhydrophobic surface through the coordination of a metallic multi-scale structure and the low surface energy of Al. In addition, the low surface energy of Al requires no additional chemical treatment, which is another advantage with respect to durability. To verify the industrial potential of the multi-scale metallic pattern presented here, film sample was prepared, as demonstrated in Figure 3c. This polymer film was produced with perfluoropolyether (PFPE) via UV-assisted capillary force lithography. As shown in Figure 3c, the metallic surface was easily replicated with the same multi-scale pattern.

Figure 4 shows the superhydrophobicity. Figure 4a represents the dynamic contact angle and hysteresis is very low at 3° . Such low hysteresis value indicates the metal surface has the hydrophobic properties. Figure 4b shows the behavior of droplet impact experiment. As shown in the image, the classical bouncing behavior takes place on the superhydrophobic surface.

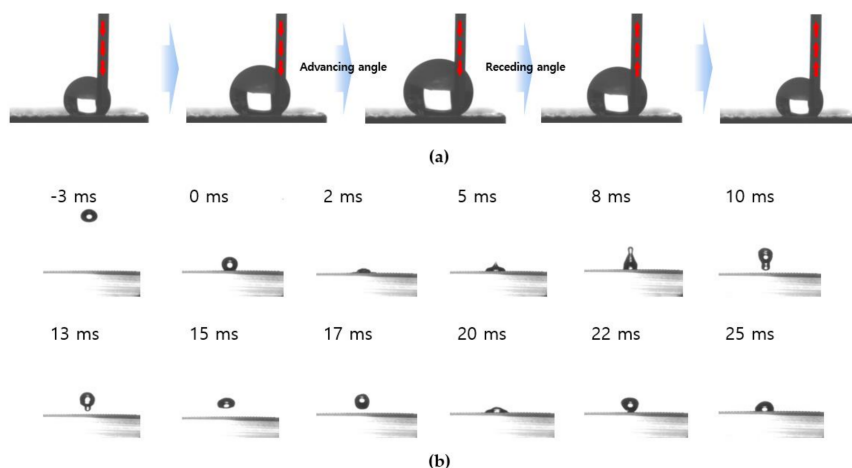


Figure 4. (a) Hysteresis and (b) time-lapsed images of water droplet shown in a superhydrophobic metal mold.

Figure 5 shows the 3D morphology and the SEM images of the multi-scale roughness on the metallic surface and the replicated polymer film. Figures 5a and 2c show 3D images (5.25 mm × 5.25 mm) of a partial metal mold and replicated polymer film, which provide a direct understanding of the 3D shape of the surface. Figure 5a shows the metal mold processed with WEDM. Figure 5c shows the replicated polymer film where a line pattern is transferred using the metal mold on the flat polymer film. The metal mold (Figure 5a) was manufactured by passing a wire electrode through a sinusoidal pathway of 500 micro wavelengths. Replicated polymer films (Figure 5c) were fabricated by transferring a pattern in the master mold via the PFPE precursor dispensed onto the surface of the metal mold under a sheet of polymer film, followed by UV exposure for 5 mins. As shown in Figure 5c, the initial morphologies are the same due to the nature of the UV-assisted capillary force lithography [26–28]. In this paper, a commercial WEDM machine was used to fabricate the micro-sized patterns and surface roughness on the workpiece.

Figure 5b show the line scan profile of the metal mold. Figure 5b shows the scanned data of the cross-section of the metal mold, whereby the film is divided into the X-axis and Y-axis (in millimeters). The top waveforms (X direction) in Figure 5b represent 500 micrometer cycles. Figure 5d shows the line scan profile of the replicated polymer film. Figure 5d shows the scanned data of the cross-section in the replicated polymer film, whereby the film is divided into the X-axis and Y-axis (in millimeters). The top waveforms (X direction) in Figure 5b represent 500 micrometer cycles. As shown in Figure 5b,d, the line scan profiles are almost identical. In the (X direction scan profile shown in Figure 5b,d, the micro-sized structures repeated at 500 micrometers are similar. Also, streamlined shapes with ripples can be seen due to the nano-sized roughness. In the Y direction scan profile of Figure 5b,d, the nano-sized roughnesses of the metal mold and polymer replica surfaces almost coincide. This indicates that the transfer of the morphology from the metal mold to the polymer film is accomplished by UV-assisted capillary force lithography.

Figure 5e,g show SEM images of the metal mold and replicated polymer film, respectively. Figure 5e shows SEM images of the metal molds with 500 μm scale bar and 250 μm scale bar. Figure 5g shows the SEM images of the replicated polymer film with 500 μm scale bar and 250 μm scale bar. Figure 5f,h show the enlarged 3D images and the arithmetical average roughness (R_a) of the metal mold and replicated polymer film, respectively. Figure 5f shows an enlarged 3D image and R_a of the metal mold. A high R_a value indicates a high surface roughness, which also indicates a large surface area. The bar graph and error bar of the R_a values in the present analysis refer to the mean value and standard deviation after the three measurements (line scan profile 1, 2, and 3) in Figure 5b. The R_a value measured in Figure 5f was 11.253 ± 2.475 μm in the (X direction and 5.025 ± 1.872 μm in the Y direction. Figure 5h shows an enlarged 3D image and R_a of the replicated polymer film. The bar graph and error bar of the R_a values in the present analysis refer to the mean value and standard deviation after the three measurements (line scan profile 1, 2, and 3) shown in Figure 5d. The R_a value measured in Figure 5h was 10.738 ± 1.978 μm in the (X direction and 4.992 ± 1.323 μm in the Y direction. The result of Figure 5 confirmed that the metal mold morphology was successfully transferred to the polymer film through UV-assisted capillary force lithography using PFPE resin. In summary, it was confirmed that the surface morphology of Figure 5e was transferred well, as in Figure 5g.

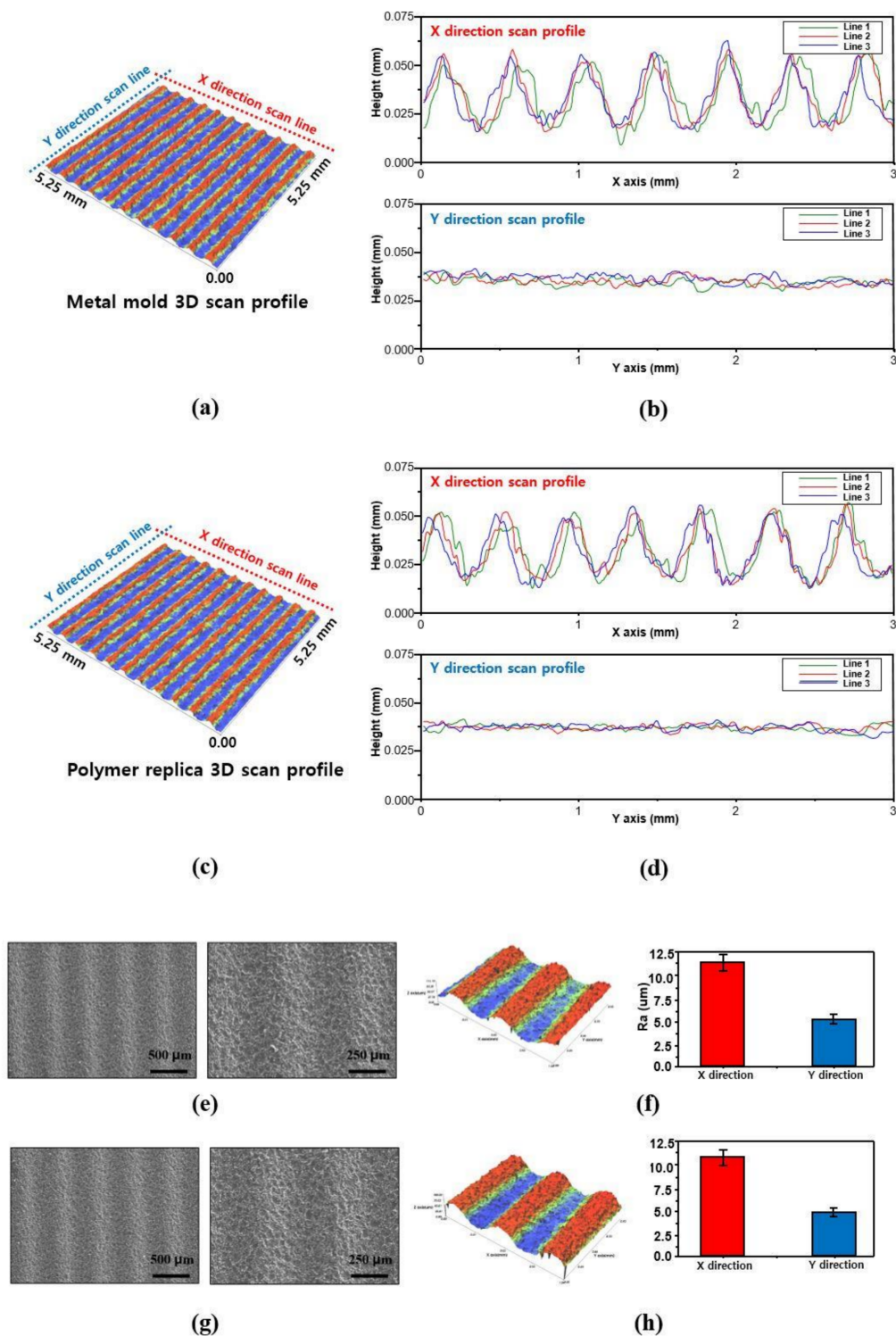
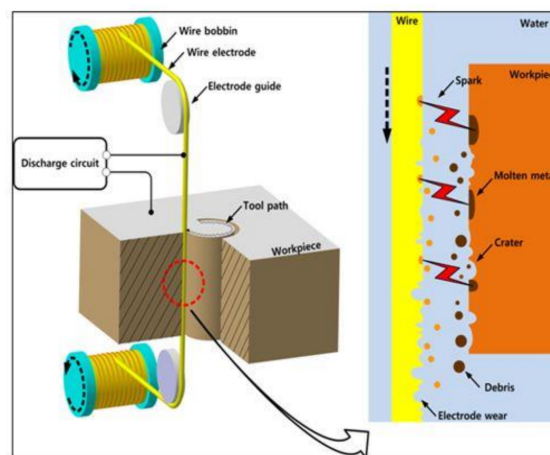


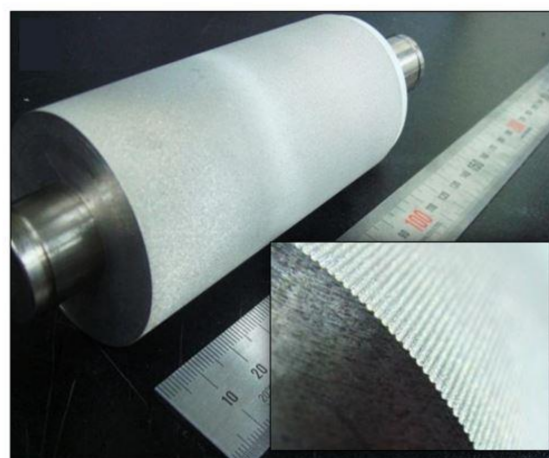
Figure 5. Fabrication of bio-inspired 3D master mold: (a) 3D image of metal mold surface after WEDM process taken by surface profiler; (b) Line scan profiles of metal mold surface in X and Y directions; (c) 3D image of polymer replica surface after WEDM process taken by surface profiler; (d) Line scan profiles of polymer replica surface in X and Y directions; (e) SEM images of metal mold surface; (f) Enlarged 3D morphology image of metal mold surface and surface roughness averages (R_a) measured in b. Error bars show the standard deviation of the three experiments; (g) SEM images of polymer replica surface; (h) Enlarged 3D morphology image of polymer replica surface and surface roughness averages (R_a) measured in (d). Error bars show the standard deviation of the three experiments.

3.2. Applications of Seamless Metal Mold for Roll-To-Roll Process

The roll-to-roll nanoimprint process has garnered attention recently because of its suitability for the high throughput manufacturing of various thin film devices, such as wire grid polarizers and solar cells [29–31]. A roll mold is generally fabricated by attaching a flexible planar polymer sheet of which the patterns are replicated from a silicon master via the conventional nanoimprint process. However, the resulting roll mold has seams, which causes a yield loss of the replicated film product. To overcome this problem, new methods that utilize self-organized structures, including block copolymer and aluminum anodic oxidation, can be used. However, it is difficult to design the pattern features and shapes using the current technology. Using WEDM, the seamless roll mold could be easily made with dual-scale roughness. A seamless patterned polymer film product with dual-scale roughness superhydrophobicity can then be obtained by roll-to-roll imprinting. The cylindrical mold was fabricated in one step as follows. The non-patterned metal substrate was initially prepared by conventional machining (bulk state) and the roll mold was then machined with a 500- μm sinusoidal wavelength using the cut process, as described previously in Figure 6a. Consequently, the roll mold spontaneously formed a dual-scale roughness with a seamless pattern and superhydrophobicity. Figure 6b shows the results of the one-step fabrication process and the cylindrical Al alloy with a diameter of 45 mm.



(a)



(b)

Figure 6. (a) Schematic diagram of WEDM process used to fabricate multi-scale patterned roll; (b) Optical images of the fabricated multi-scale patterned roll for roll-to roll process.

Figure 7 shows a schematic illustration of the roll-to-roll process using a multi-scale patterned seamless mold in which a nanoimprint lithography technique using UV-curable resin was used for the pattern replication.

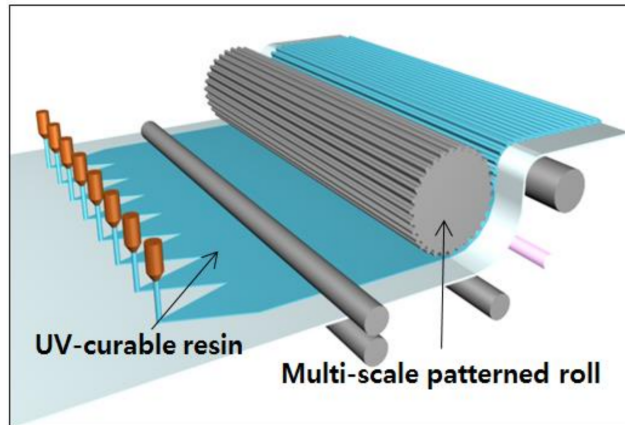


Figure 7. Schematic illustration of roll-to-roll process used to produce superhydrophobic polymer film with a WEDM-machined metallic roll.

Finally, roll-to-roll nanoimprint patterning was carried out using local equipment, as shown in Figure 8. In the roll-to-roll printing, a polyethylene terephthalate (PET) substrate coated with UV-curable resin was placed in the equipment. The lower back-up transfer roller was rotated at 1 rpm, and the PET film was exposed to UV light ($\lambda = 250\text{--}400\text{ nm}$, dose = $300\text{ mJ}/\text{cm}^2$). After the PET substrate was run through the patterned roll mold, the dual-roughness pattern was replicated onto the cured PFPE resin on the PET support within a few seconds [26,32,33].

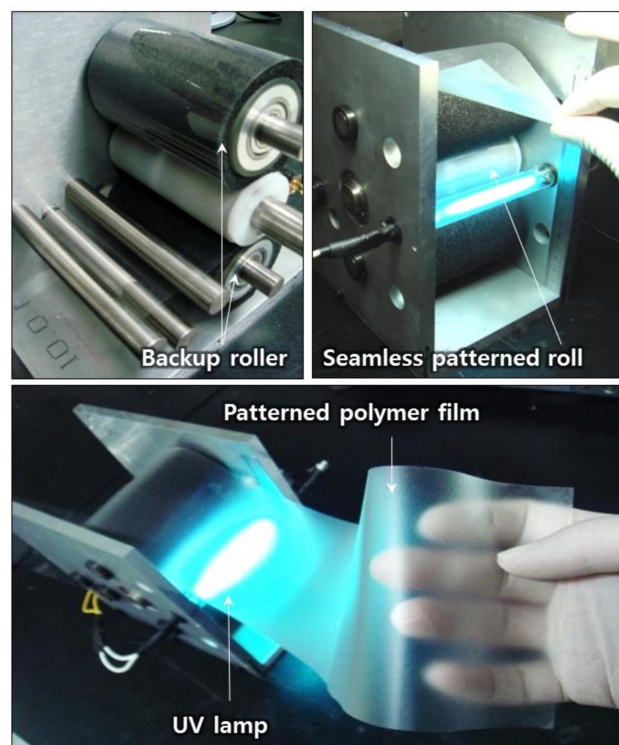


Figure 8. Digital pictures showing the roll-to-roll equipment and an example of replicated superhydrophobic polymer film.

Figure 9 shows the replicated surface morphology of the polymer film formed on the metallic roll mold surface. Figure 9a shows 3D images (5.25 mm \times 5.25 mm) of the partially replicated polymer film after the roll-to-roll process, providing a direct understanding of the 3D shape of the surface. Figure 9b shows a line scan profile of the replicated polymer film after the roll-to-roll process. Figure 9b shows the scanned data of the cross-section in the replicated polymer film in which the film is divided into the X-axis and Y-axis (millimeters). The top waveforms (X direction) in Figure 9b represent 500 micrometer cycles. Figure 9c shows a SEM image of the polymeric replica with the inset showing a nano-sized surface roughness. It can be confirmed that the morphology of the metal mold was successfully transferred to a replicated polymer film using a roll-to-roll method, since Figure 9a–c are similar to Figure 5a,b,e, respectively. Figure 9d shows the transmittance property of the replicated polymer film with the inset showing water droplets on the replicated polymer film.

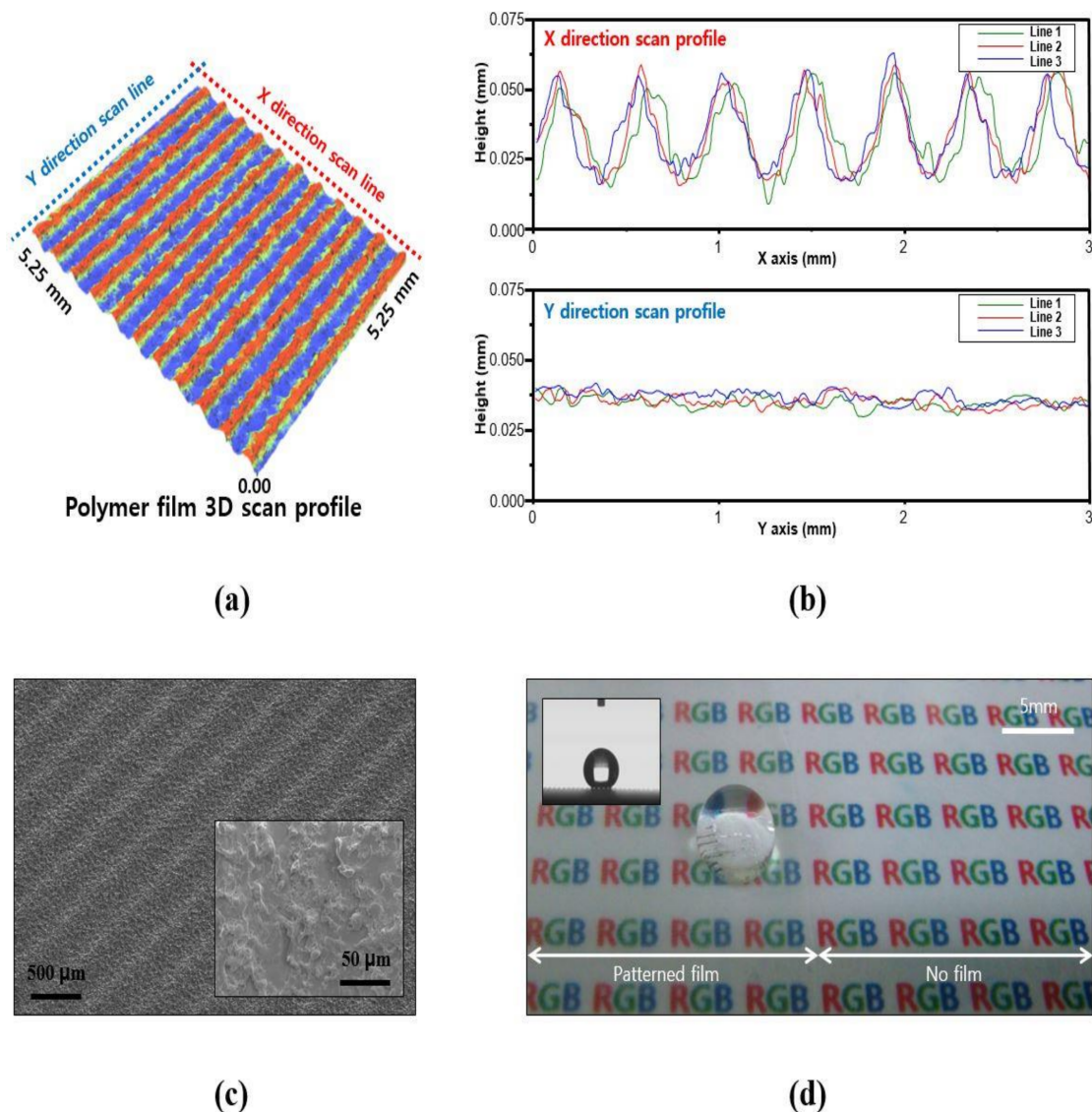


Figure 9. (a) Replicated polymer film corresponding to the 3D morphology image with multi-scale roughness after roll-to-roll process; (b) Line scan profiles of replicated polymer film surface in X and Y directions; (c) SEM image of replicated polymer film surface with multi-scale roughness after roll-to-roll process; (d) Transmittance property of replicated polymer film.

The water contact angle was 150° , indicating a superhydrophobic surface. The transmittance property of the film was confirmed to be very high by comparing the presence and absence of the film. Also, it was shown that the contact angle was very high at 150° , indicating that the roll-to-roll process accurately transferred the morphology of the metal mold to ensure superhydrophobic properties. Figure 9 shows that the replicated polymer film has a very high transmittance property and hydrophobic property. In addition, the roll-to-roll method allows the large-area production of replicated polymer films. Therefore, the replicated polymer film production by the roll-to-roll method is applicable to fields with applications, including wire grid polarizers and solar cells, where the transmittance property and hydrophobic property should be high and large area production should be possible.

4. Conclusions

In this paper, a seamless roll mold applicable for roll-to-roll processing of aluminum (Al) was fabricated through the WEDM process. The surface of the seamless roll mold has dual-roughness and exhibits a superhydrophobic characteristic. Patterns of hundreds of micrometer scale can be made on the surface of the Al using the WEDM process and a roughness ranging from several micrometers to one hundred nanometers is generated naturally on the surface of the steel due to the characteristic of EDM process. The dual-roughness surface manufactured in this way exhibits a superhydrophobic characteristic without additional chemical coating. Al has low surface energy, which positively affects superhydrophobicity and enables it to be used as a replica mold. This is because the dual-roughness on the surface of the Al can be easily reproduced using polymer films without additional surface treatment. Al can be easily transformed into a seamless cylindrical shape through the WEDM process. If hundreds of micrometer patterns are engraved on the surface of the cylinder, a roll mold with seamless dual-roughness can be fabricated. If the dual-roughness on the surface of a seamless roll mold is transcribed to a polymer film by the roll-to-roll process, a superhydrophobic film with a large area can be produced. This large-scale fabricated superhydrophobic film that is presented in this paper is applicable to the architecture or automobile windows, eyeglasses, and optical windows for electronic devices. On top of that, it also can be used in many fields such as fluidic drag reduction, anti-biofouling, and prevention of water corrosion.

Acknowledgments: This research was supported by Nano Material Technology Development Program through the National Research Foundation of Korea (NRF) funded by the Ministry of Science, ICT and Future Planning. (2009-0082580) and also this work was supported by the Soongsil University Research Fund of 2016.

Author Contributions: Won-Gyu Bae conceived and designed the research, conducted the experiments and prepared the draft manuscript. Jin-Young So performed data analysis and participated in the discussions.

Conflicts of Interest: The authors declare no conflict no interest.

References

1. Xia, F.; Jiang, L. Bio-inspired, smart, multiscale interfacial materials. *Adv. Mater.* **2008**, *20*, 2842–2858. [[CrossRef](#)]
2. Liu, K.; Yao, X.; Jiang, L. Recent developments in bio-inspired special wettability. *Chem. Soc. Rev.* **2010**, *39*, 3240–3255. [[CrossRef](#)] [[PubMed](#)]
3. Chu, W.-S.; Lee, K.-T.; Song, S.-H.; Han, M.-W.; Lee, J.-Y.; Kim, H.-S.; Kim, M.-S.; Park, Y.-J.; Cho, K.-J.; Ahn, S.-H. Review of biomimetic underwater robots using smart actuators. *Int. J. Precis. Eng. Manuf.* **2012**, *13*, 1281–1292. [[CrossRef](#)]
4. Bae, W.G.; Kim, H.N.; Kim, D.; Park, S.H.; Jeong, H.E.; Suh, K.Y. 25th anniversary article: Scalable multiscale patterned structures inspired by nature: The role of hierarchy. *Adv. Mater.* **2014**, *26*, 675–700. [[CrossRef](#)] [[PubMed](#)]
5. Yao, X.; Song, Y.; Jiang, L. Applications of bio-inspired special wettable surfaces. *Adv. Mater.* **2011**, *23*, 719–734. [[CrossRef](#)] [[PubMed](#)]

6. Liu, K.; Jiang, L. Bio-inspired design of multiscale structures for function integration. *Nano Today* **2011**, *6*, 155–175. [[CrossRef](#)]
7. Li, X.-M.; Reinhoudt, D.; Crego-Calama, M. What do we need for a superhydrophobic surface? A review on the recent progress in the preparation of superhydrophobic surfaces. *Chem. Soc. Rev.* **2007**, *36*, 1350–1368. [[CrossRef](#)] [[PubMed](#)]
8. Nakajima, A.; Hashimoto, K.; Watanabe, T. Recent studies on super-hydrophobic films. *Monatsh. Chem.* **2001**, *132*, 31–41. [[CrossRef](#)]
9. Abbas, N.M.; Solomon, D.G.; Bahari, M.F. A review on current research trends in electrical discharge machining (EDM). *Int. J. Mach. Tools Manuf.* **2007**, *47*, 1214–1228. [[CrossRef](#)]
10. Shin, H.S.; Park, M.S.; Chu, C.N. Machining characteristics of micro EDM in water using high frequency bipolar pulse. *Int. J. Precis. Eng. Manuf.* **2011**, *12*, 195–201.
11. Kim, Y.-T.; Park, S.-J.; Lee, S.-J. Micro/meso-scale shapes machining by micro EDM process. *Int. J. Precis. Eng. Manuf.* **2005**, *6*, 5–11.
12. Puthumana, G.; Joshi, S.S. Investigations into performance of dry EDM using slotted electrodes. *Int. J. Precis. Eng. Manuf.* **2011**, *12*, 957–963. [[CrossRef](#)]
13. Shin, H.S.; Kim, B.H.; Chu, C.N. High frequency micro wire EDM for electrolytic corrosion prevention. *Int. J. Precis. Eng. Manuf.* **2011**, *12*, 1125–1128.
14. Yoo, B.H.; Min, B.-K.; Lee, S.J. Analysis of the machining characteristics of EDM as functions of the mobilities of electrons and ions. *Int. J. Precis. Eng. Manuf.* **2010**, *11*, 629–632. [[CrossRef](#)]
15. Han, F.; Jiang, J.; Yu, D. Influence of machining parameters on surface roughness in finish cut of WEDM. *Int. J. Adv. Manuf. Technol.* **2007**, *34*, 538–546. [[CrossRef](#)]
16. Rao, P.S.; Ramji, K.; Satyanarayana, B. Effect of wedm conditions on surface roughness: A parametric optimization using taguchi method. *Int. J. Adv. Eng. Sci. Technol.* **2011**, *6*, 41–48.
17. Kiyak, M.; Cakır, O. Examination of machining parameters on surface roughness in EDM of tool steel. *J. Mater. Process. Technol.* **2007**, *191*, 141–144. [[CrossRef](#)]
18. Starke, E.; Staley, J. Application of modern aluminum alloys to aircraft. *Prog. Aerosp. Sci.* **1996**, *32*, 131–172. [[CrossRef](#)]
19. Immarigeon, J.; Holt, R.; Koul, A.; Zhao, L.; Wallace, W.; Beddoes, J. Lightweight materials for aircraft applications. *Mater. Charact.* **1995**, *35*, 41–67. [[CrossRef](#)]
20. Bae, W.G.; Song, K.Y.; Rahmawan, Y.; Chu, C.N.; Kim, D.; Chung, D.K.; Suh, K.Y. One-step process for superhydrophobic metallic surfaces by wire electrical discharge machining. *ACS Appl. Mater. Interfaces* **2012**, *4*, 3685–3691. [[CrossRef](#)] [[PubMed](#)]
21. Lee, Y.; Park, S.H.; Kim, K.B.; Lee, J.K. Fabrication of hierarchical structures on a polymer surface to mimic natural superhydrophobic surfaces. *Adv. Mater.* **2007**, *19*, 2330–2335. [[CrossRef](#)]
22. Liu, X.H.; Zhang, L.Q.; Zhong, L.; Liu, Y.; Zheng, H.; Wang, J.W.; Cho, J.-H.; Dayeh, S.A.; Picraux, S.T.; Sullivan, J.P. Ultrafast electrochemical lithiation of individual Si nanowire anodes. *Nano Lett.* **2011**, *11*, 2251–2258. [[CrossRef](#)] [[PubMed](#)]
23. Ma, M.; Hill, R.M.; Rutledge, G.C. A review of recent results on superhydrophobic materials based on micro-and nanofibers. *J. Adhes. Sci. Technol.* **2008**, *22*, 1799–1817. [[CrossRef](#)]
24. Guo, Z.; Zhou, F.; Hao, J.; Liu, W. Stable biomimetic super-hydrophobic engineering materials. *J. Am. Chem. Soc.* **2005**, *127*, 15670–15671. [[CrossRef](#)] [[PubMed](#)]
25. Qu, M.; Zhang, B.; Song, S.; Chen, L.; Zhang, J.; Cao, X. Fabrication of superhydrophobic surfaces on engineering materials by a solution-immersion process. *Adv. Funct. Mater.* **2007**, *17*, 593–596. [[CrossRef](#)]
26. Suh, K.Y.; Kim, Y.S.; Lee, H.H. Capillary force lithography. *Adv. Mater.* **2001**, *13*, 1386. [[CrossRef](#)]
27. Bruinink, C.M.; Péter, M.; Maury, P.A.; De Boer, M.; Kuipers, L.; Huskens, J.; Reinhoudt, D.N. Capillary force lithography: Fabrication of functional polymer templates as versatile tools for nanolithography. *Adv. Funct. Mater.* **2006**, *16*, 1555–1565. [[CrossRef](#)]
28. Tamaki, Y.; Kataoka, Y.; Miyazaki, T. Bone regenerative potential of mesenchymal stem cells on a micro-structured titanium processed by wire-type electric discharge machining. *arXiv* **2010**.
29. Ahn, S.H.; Guo, L.J. High-speed roll-to-roll nanoimprint lithography on flexible plastic substrates. *Adv. Mater.* **2008**, *20*, 2044–2049. [[CrossRef](#)]
30. Krebs, F.C.; Gevorgyan, S.A.; Alstrup, J. A roll-to-roll process to flexible polymer solar cells: Model studies, manufacture and operational stability studies. *J. Mater. Chem.* **2009**, *19*, 5442–5451. [[CrossRef](#)]

31. Bae, S.; Kim, H.; Lee, Y.; Xu, X.; Park, J.-S.; Zheng, Y.; Balakrishnan, J.; Lei, T.; Kim, H.R.; Song, Y.I. Roll-to-roll production of 30-inch graphene films for transparent electrodes. *Nat. Nanotechnol.* **2010**, *5*, 574–578. [[CrossRef](#)] [[PubMed](#)]
32. Suh, K.Y.; Park, M.C.; Kim, P. Capillary force lithography: A versatile tool for structured biomaterials interface towards cell and tissue engineering. *Adv. Funct. Mater.* **2009**, *19*, 2699–2712. [[CrossRef](#)]
33. Jeong, H.E.; Kwak, M.K.; Park, C.I.; Suh, K.Y. Wettability of nanoengineered dual-roughness surfaces fabricated by UV-assisted capillary force lithography. *J. Colloid Interface Sci.* **2009**, *339*, 202–207. [[CrossRef](#)] [[PubMed](#)]



© 2018 by the authors. Licensee MDPI, Basel, Switzerland. This article is an open access article distributed under the terms and conditions of the Creative Commons Attribution (CC BY) license (<http://creativecommons.org/licenses/by/4.0/>).